Cheating the Cheaters:

Spatial Dynamics in the Evolutionary Stability of Antibiotic Resistance

Devin Akman[1], LeMar Callaway III[2], Pablo Cárdenas[3], Joshua Nieve–Silva[4], Jun Chen[5], Baltazar Espinoza[5], Leon Arriola[6], and Carlos Castillo-Garzow[7]

[1] *University of Illinois, Urbana–Champaign, IL, USA*

[2] *Virginia Wesleyan University, Virginia Beach, VA, USA*

[3] *Universidad de Los Andes, Bogotá, Colombia*

[4] *Montclair State University, Montclair, NJ, USA*

[5] *Arizona State Univerisity, Tempe, AZ, USA*

[6] *University of Wisconsin, Whitewater, Whitewater, WI, USA*

[7] *Eastern Washington University, Cheney, WA, USA*

Abstract

Infections caused by antibiotic–resistant bacteria are posed to be one of the most pressing health concerns of the twenty–first century. A common mechanism of resistance involves production of an antibiotic–degrading enzyme. In this case, neighboring, nonproducer bacteria can "cheat" by sharing the benefits of resistance while the metabolic cost of enzyme production falls solely on producer cells. The objective of this work is to explore how the spatial population dynamics of producers and nonproducer maintain the resistance found in biofilms. A three–dimensional spatial model was used to simulate growth of both producers and nonproducer under antibiotics with different characteristics. Standard antibiotics resulted in a heterogeneous populations with stable, homogeneous community structure. The population of resistant bacteria was most sensitive to altering the fitness cost of enzyme production. These results could suggest novel antibacterial treatments in order to create therapies less likely to favor the evolution of resistance.

1 Introduction

Throughout most of human history, infectious diseases have been the second leading cause of death among individuals, with bacteria playing a central role [1]. Clinicians now face the obstacle of antibiotic–resistant bacterial disease. If neglected, this new menace is posed to undo much of what clinicians have accomplished, leaving millions at risk [1]. The driving force behind resistance is the selection pressure imposed by the use of antibiotics, which results in resistance to antibiotics becoming an evolutionary stable strategy for bacteria. The purpose of this research is to analyze the dynamics of a bacterial population in order to find ways to destabilize the strategy of resistance. According to the hypothesis being proposed, this could be done by finding conditions favorable for the proliferation of bacteria that do not contribute to the resistance of the population, as shall be explained in the following pages. Should the hypothesis hold true, it could suggest new treatment approaches against resistant strains of bacteria and preventive strategies that avoid their appearance in the first place.

1.1 Historical Background

While not as apparent today, the pre–antibiotic era was marked with outbreaks of bacterial diseases such as cholera, bubonic plague, tuberculosis, and leprosy, claiming hundreds of thousands of lives [1, 2]. Bacterial infection of open wounds and childbirth lesions were an ordinary phenomenon [2]. Occurrences of outbreaks continued to escalate throughout the industrial revolution. As explained in [3], mass immigration to American cities introduced new viral/bacterial strains into a susceptible population. Cramped city housing allowed for the easy transmission of said diseases. Inadequate waste management systems, coupled with poor public health services, hindered any recovery efforts. Under these conditions, the main causes of death in the United States at the start of the twentieth century were tuberculosis, influenza and diarrhea [4]. The relevance of bacterial disease was a situation representative of most of the world at the time [2].

As a result, resources, time, and study have been allocated to the understanding and eradication of such illnesses. Interactions between bacterial diseases and human response have introduced therapies adept in fighting infection. One such treatment that has revolutionized how clinicians combat bacterial disease has been the use of antibiotics. Beginning with the large–scale implementation of penicillin in 1942 [1], numerous classes of antibiotics have been discovered and used to treat bacterial illness.

The initial effectiveness of antibiotics created a culture overly dependent on their use. Although it is true that excessive prescription, patient misuse, and overuse of antibiotics in the livestock industry have contributed to the rapid spread of resistance [5], it is a problem that underlies the way antibiotics

are designed to be used. Antibiotics, when conceived as tools to try to completely erradicate every member of a population of bacteria, constitute a strong evolutionary selection pressure favoring the growth of resistant bacteria. The stronger the selection pressure, the more evolutionary incentive bacteria will have to be resistant. Proof of this is the speed with which resistance to an antibiotic is found. Penicillin–resistant strains of bacteria were widely found in hospitals throughout the 1950s [6]. Methicillin, the next–generation replacement of penicillin and its derivatives, was met with resistant strains in 1962, a year after being introduced into hospitals [6]. All classes of antibiotics introduced into clinical use since then have followed similar trends, with resistance being encountered a few years after being introduced, or even before doing so [6]. This goes to show the importance of reconsidering the view of antibiotics as "weapons of mass destruction" at a microbial scale, in favor of a more nuanced view of them as "precision weapons" aimed at modifying bacterial population dynamics.

1.2 Resistance Strategies Taken by Bacteria

In order to understand how to use antibiotics as "precision weapons", it is necessary to understand how resistance works. Resistant bacteria have developed numerous strategies to neutralize the threat of antibiotics. One strategy often employed is the formation of a biofilm on the surface of a substrate. Biofilms are composed of dense concentrations of bacteria embedded in an extracellular matrix composed of substances synthesized by the microorganisms [7]. They are common in natural environments, but they constitute a significant challenge in clinical situations [8]. Bacteria in biofilms are known to be significantly more resistant to antibiotic treatment than their free–living, planktonic counterparts, even in situations in which they are genetically identical to each other [7]. Multiple mechanisms have been proposed to explain this, including reduced diffusion rates of antibiotic in biofilm, slower metabolic rates, and degradation of the antibiotic in the extracellular matrix [7, 9]. Nevertheless, fluorescent microscopy studies have found that diffusion of small molecules occurs throughout biofilms in a matter of hours [10], leading authors to conclude reduced antibiotic diffusion is not the principal means by which biofilms increase antibiotic resistance [10, 7, 11]. Therefore, the latter two mechanisms of antibiotic degradation and slow metabolism are of particular interest to this study.

Antibiotics can have various modes of actions and can disrupt biological processes at various stages in the bacterial life cycle, including protein synthesis, nucleic acid synthesis or cell wall synthesis [12]. Given that all of these processes depend on the metabolic rate of a given bacterium, the effectiveness of the antibiotic is reduced in conditions of low metabolism. Well–known examples of this are β–lactam antibiotics such as penicillin or piperacillin, which function as inhibitors for cell wall biosynthesis [13].

These antibiotics hinder the biosynthesis process by competitively binding and irreversibly inhibiting enzymes responsible for catalyzing the polymerization of peptidoglycan, an essential polymer in preserving the structural integrity of a cell wall [13]. In an environment where β–lactam are not present, biosynthesis is undeterred; however, once introduced, the antibiotic binds to DD-transpeptidase, preventing peptidoglycan production [13]. Consequently, the cell wall degrades, leaving a fragile spheroplast which dies soon after [13]. However, if a bacterium is undergoing growth and replication at a slower rate, cell wall synthesis is less likely to occur, and the death rate due to antibiotic presence is reduced. Measurement of growth rate inside biofilms have shown replication rates up to ten times slower for bacteria at the bottom of the biofilm when compared to surface–dwellers, probably due to reduced levels of resources available in the highly–dense areas at the bottom of the biofilm [14].

Another common mechanism of resistance amplified within biofilms involves the secretion of enzymes outside the cell wall that degrade the antibiotic. An example of such a mechanism is the release of β–lactamases from a β–lactam resistant bacteria [15, 16]. This production is activated by an increase in wall precursor molecules inside the cell wall [16]. As the β–lactam is inhibiting cell wall synthesis, the concentration of wall precursors such as murein increases until the activation level is reached. A signal transduction cascade activated by the increased concentration of precursors results in the expression of β–lactamase genes inside the cell, producing β–lactamases [16]. The enzyme is then secreted from the cell, where it then comes in contact with the β–lactam antibiotic. This interaction results in the hydrolysis of the β–lactam ring, and the antibiotic is rendered ineffective for treatment. As the antibiotic concentration decreases, so does the concentration of wall precursors that are now used as structural support for the cell wall. When the concentration falls below the activation level, expression of β–lactamases halts [16]. However, antibiotic will readily diffuse from the surroundings towards the surface of the enzyme–producing bacterium, inducing β–lactamase production. This negative–feedback regulation system results eventually reaches equilibrium levels of antibiotic degradation and gene expression, and thus metabolic cost. In this work, bacteria that produce degradation enzymes in this manner are denominated "producers", while those that do not are "nonproducers".

1.3 Benefits and Costs of Resistance by Enzyme Production

This process highlights several key features necessary in studying the interactions of bacterial cells in a biofilm. First, the benefits of antibiotic degradation are also shared by neighboring, nonproducer bacteria. Each producer bacterium found can be thought of as a point sink with a constant flux of antibiotic toward it, causing a decreased concentration of antibiotics around it at equilibrium [9]. The

result is a decrease in antibiotic concentration near the sinks when compared to the concentration elsewhere. Thus, nonproducer bacteria near the vicinity of producers are surrounded with a lower concentration of antibiotics than if they were far from any producer bacteria. Consequently, their relative fitness increases compared to other cells increases [17].

Furthermore, producer bacteria only produce the amount of enzyme necessary to ensure their own survival, as explained above. Such behavior encourages cooperation between producer bacteria close enough to each other for their antibiotic degradation to impact each other's local antibiotic concentration. Therefore, the producer bacterial cells involved produce less enzyme than if they were isolated. This implies varying fitness levels, where close–knit groups of resistant bacteria are more fit than separated resistant cells or clumps of nonresistant cells.

Despite the shared benefits resistance has on the local bacterial community, costs are administered unevenly. Bacterial cells that are resistant pay for their resistance with decreased metabolic rates and functions [18, 17]. Studies have shown resistant cells expend large resources of energy in producing the proteins required to maintain resistance [18]. According to this study, when compared to nonresistant bacterial cells, they produced far less proteins used for primary metabolic functions. Moreover, the resistant strains were found to replicate at a lower rate than those who were nonresistant [18].

1.4 Spread of Resistance

Bacterial genetics play an important role in the rise and spread of resistance. Resistance genes, such as those encoding degradation enzymes, are contained within plasmids, circular units of extrachromosomal DNA. When a producer cell undergoes replication through binary fission, boeth daughter cells will usually receive a copy of the plasmid. Nevertheless, occasionally, only one of these daughter cells will receive the plasmid necessary for production of resistance [19, 20]. Instead of just passing a resistance plasmid to the next generation, bacterial cells can also spread resistance through horizontal gene transfer [21]. This mechanism can be accomplished through a number of ways, including bacterial conjugation, transformation, and transfection. Conjugation involves both a donor and recipient cell exchanging plasmids through, a hair–like organelle termed pilus [22]. Transformation occurs when bacteria uptake free nucleic acids in the medium [21]. Transfection occurs when bacteria–infecting viruses, termed bacteriophages, transfer genetic information from one cell to another [21]. In these ways, the genes for resistance can spread throughout a bacterial population.

1.5 Previous Models Studied

Previous work on microbial population dynamics has provided valuable insight for the structure and assumptions of this model. For example, Szilágyi et al. [23] examined the population dynamics of a free–living community of bacteria using game theory to model a rock–paper–scissors dynamic. A public good is a product produced by an individual that nearby individuals can benefit from [23]. Bacteria that are susceptible to the antibiotic, but are unable to produce enzymes to keep themselves safe, may hide in the safety radius of an enzyme producing bacteria without incurring the metabolic cost of producing the enzyme themselves. Szilágyi et al. [23] examined the role of these public goods, as they modeled the interactions between bacteria that produced them. The three groups considered in these models were antibiotic–producing bacteria (producers), bacteria that degrade antibiotics but do not produce them (production cheaters), and bacteria that neither produced nor degraded antibiotics (degradation cheaters). This scenario led to a rock paper scissors dynamic, similar to the scenario modeled by Inglis et al. [24]. Their work also identified conditions that lead to the collapse of the bacterial community. If a well mixed population of bacteria is invaded by production cheaters, the population equilibrium will be disrupted and a loss of a competing species due to the invasion results in decreased biodiversity [23].

The work of Szilágyi et al. [23] has shortcomings for the clinical context in different fronts. First, Szilágyi et al. [23] modeled the population with a system of ordinary differential equations, which may not accurately capture the spatial dynamics of the biofilm. Second, the three–player dynamics of free–living communities are replaced by two–player dynamics in clinical contexts, given that in pathological biofilms, the antibiotic is administered externally and not produced internally. The model studied here takes into account how the spatial organization of the biofilm affects antibiotic diffusion and population dynamics, as well as how the surrounding concentration of externally–applied antibiotic affects the fitness and reproduction rate of a given bacterium.

2 Methods

2.1 Model Parameters

Antibiotic resistance has been the subject of extensive empirical study, both *in vitro* and *in vivo*. Consequently, there is a rich source of literature from which to find values for biological constants and parameters. The model was calibrated using parameters from *Pseudomonas aeruginosa* biofilms, of high importance in the clinical setting [7], and a common *beta*–lactam antibiotic used to treat it,

piperacillin. Table 1 illustrates constant parameters used in the present model. Table 2 illustrates parameters that were varied in the analysis of the model, with their ranges of interest.

Table 1: Physical and Biological Constants

Constant	**Symbol**	**Value**	**Units**	**Reference**
Death rate in the absence of antibiotic	γ_n	$1 \cdot 0.05$	hr^{-1}	[25]
Distance between cell centers in highly dense biofilm	d_b	1.75	µm	[26]
Fraction of total body water at which antibiotic diffusion becomes negligible	β_C	0.95	–	–
Loss rate at replication of enzyme–production plasmid	λ_L	$1 \cdot 10^{-5}$	$\text{cell}^{-1} \cdot \text{hr}^{-1}$	[27]
Radius of bacteria, average	r_c	0.500	µm	[26]
Replication rate of nonproducer bacteria in the absence of antibiotic	α_n	0.909	hr^{-1}	[14]
Simulation plane length and width	X_{max}	100	µm	–
Simulation time step	t_s	1.0	hr^{-1}	–
Simulation time, maximum value	t_{max}	62	hr^{-1}	–
Thickness of cell cluster in biofilm, maximum value	Z_{max}	10.0	µm	[28]
Total body mass	M	70	kg	[29]
Total body water	V_w	5.5	L	[29]
Transfer rate at replication of enzyme–production plasmid	λ_T	$1 \cdot 10^{-5}$	$\mu\text{m}^3 \cdot \text{cell}^{-1} \cdot \text{hr}^{-1}$	[30]

Table 2: Biological and Pharmacological Control Parameters

Parameter	**Symbol**	**Range**	**Units**	**Reference**
Biofilm thickness, initial value as a fraction of maximum value	h_i	0.05	–	[31]
Clearance rate of antibiotic from blood plasma	K_a	10.02	L hr^{-1}	[32]
Minimum Inhibitory Concentration (MIC) of antibiotic for total growth inhibition in susceptible bacteria	C_M	32 (piperacillin)	$\mu g\, mL^{-1}$	[33]
Minimum Inhibitory Concentration (MIC) of antibiotic for 50% growth inhibition (MIC_{50})	C_I	4 (piperacillin)	$\mu g\, mL^{-1}$	[33]
Concentration of antibiotic at cell wall of resistant bacteria	C_c	[0.001,100]	$\mu g\, mL^{-1}$	–
Proportion of resistant bacteria in biofilm, initial	ϕ_i	0.001	$cells^{-1}$	[34]
Relative fitness of enzyme producers to nonproducer in absence of antibiotic	F_E	0.8696	hr^{-1}	[17]
Set of antibiotic doses administered	D	[80,100]	$mg\, kg^{-1}$	[35]
Set of times at which doses of antibiotic are administered	T	[4,6,8,12+]	hr^{-1}	[35]

2.2 Model Design

The model studied is a spatially explicit, probabilistic, three–dimensional simulation of individual bacteria across discrete time. Each bacterium had a distinct location, and belonged to either one of two classes: enzyme–producing resistant bacterium (producers), or non enzyme–producing bacteria (nonproducer). Information relevant to a bacterium's survival and reproduction was stored for each bacterium, including its production class, the local antibiotic concentration, and the total number and location of nearby neighbors. Bacteria, simplified as spheres, are considered static in space, an assumption based on experimental evidence of low cell mobility inside the biofilm [36]. At every

time step, every bacterium can undergo one of three different actions: replication through binary fission, death due to the action of the antibiotic or natural causes, and horizontal gene transfer of the gene encoding the antibiotic–degrading enzyme. Figure 1 illustrates the various actions routes any one bacteria can take at a given time step. Bacteria may either die through natural causes, acquire resistance plasmids through horizontal gene transfer, or attempt replication. Once replication is attempted, they may either complete binary fission successfully, die due to the antibiotic's effect if they are not producers, or segregate the enzyme–production plasmid to only one daughter cell if they are producers. The actions undertaken modify environmental conditions –namely, local concentration of antibiotic and local population density– experienced by both the bacterium in question and its neighbors. These conditions go on to modify the future behavior of all the bacteria in the vicinity.

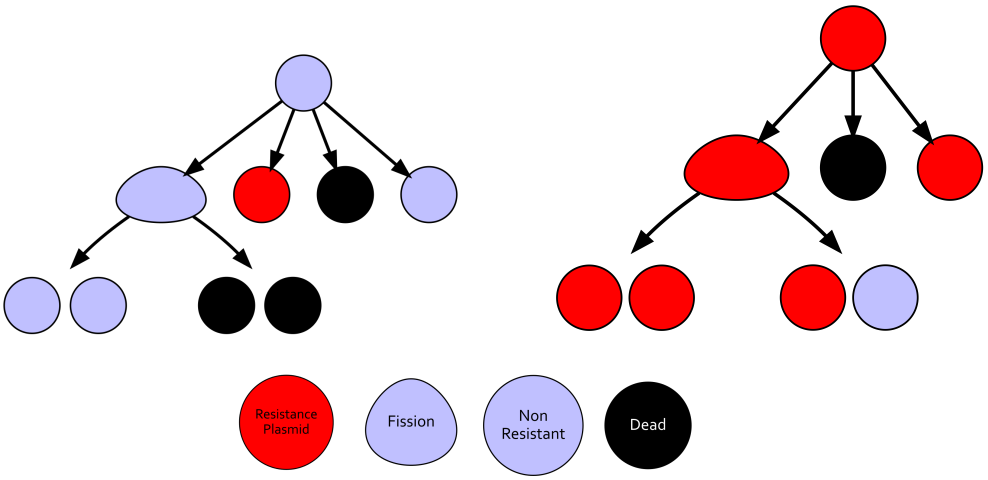

Figure 1: Different possible actions a nonproducer (left) and producer (right) bacterium can undertake in one time step. Bacteria may either die through natural causes, acquire resistance plasmids through horizontal gene transfer, or attempt binary fission, which may result in successful replication or antibiotic–induced death.

2.3 Antibiotic Dynamics and Effects

2.3.1 Total Body Water Antibiotic Concentration

The local concentration of antibiotic impacts a bacterium's probability of death and is therefore crucial to calculate in the model developed. It is assumed all of the mass of antibiotic in the dose enters total body water immediately upon administration, for example as occurs in intravenous administration, resulting in a maximum peak concentration given by $C_{B,peak}$:

$$C_{B,peak} = D(t)\frac{M}{V_w} \tag{1}$$

At the body–system level, the model assumes the antibiotic diffuses freely throughout the total body water of the patient, and is removed through renal excretion at a rate of $\gamma_a = K_a/V_w$ [37]. This means the concentration in total body water follows an exponential decay between time steps, with new doses of concentration $D(t)$ being administered at specific time points $t \in T$. Thus, the concentration $C_B(t)$ of antibiotic in total body water at time t is given in terms of the concentration $C_{B,peak}$ and the time $t_{B,peak}$ at the last dosage peak by:

$$C_B(t) = \begin{cases} C_{B,peak} \cdot \exp\left(-\gamma_a(t - t_{B,peak})\right) & t \notin T \\ C_{B,peak} \cdot \exp\left(-\gamma_a(t - t_{B,peak})\right) + D(t) & t \in T \end{cases} \tag{2}$$

2.3.2 Local Antibiotic Diffusion Dynamics in Biofilm

At the local level of the biofilm, fluorescent microscopy studies have found that small molecules such as antibiotics (200 to 500 Da, [38]) diffuse freely throughout the biofilm [39, 7]. Therefore, to simplify diffusion phenomena, it is assumed the concentration of antibiotic in the biofilm is in temporal equilibrium with the concentration in the total body water at each timestep. This means the concentration of antibiotic at any point inside the biofilm is dictated by the conditions at that timestep, without regard of the system's previous state.

On the other hand, large molecules like antibiotic–degrading enzymes (30 to 40 kDa) have negligible diffusion inside cell clusters in a biofilm [40], justifying the treatment of producer cells as point sinks of antibiotic. Because these enzymes lose efficacy over time in the extracellular milieu [41], producer bacteria constantly express and regulate these genes in order to maintain survivable conditions without incurring in unnecessary metabolic cost [42]. This means that antibiotic degradation will occur at a constant rate at each producer cell surface, maintaining a constant concentration of enzyme and antibiotic C_c at the cell surface and necessitating a constant metabolic effort. Thus, at the temporal equilibrium occurring at every time step, there will be a concentration gradient around a producer bacterium going from C_c to C_b, described by Fick's second law of diffusion [43]. This law states that

$$\frac{\partial C}{\partial t} = D\Delta C, \tag{3}$$

where C is the concentration of a substance as a function of time and position. At equilibrium, this reduces to

$$\Delta C = 0. \tag{4}$$

Since the equilibrium concentration field is a harmonic function, a domain and boundary conditions must be defined for a unique solution. One assumption of the model is local isotropy, which necessitates radial symmetry in the solution. It then becomes natural to work in spherical coordinates with angular arguments suppressed. The general radially symmetric solution to Equation 4 is given by

$$C(r) = \frac{A}{r} + B, \tag{5}$$

where A and B are arbitrary constants. This function increases without bound at the origin (clearly, $A \neq 0$ unless $C_b = C_c$), so a sphere of radius r_c should be excluded from the domain. Let $C(r_c) = C_c$ and define the asymptotic boundary condition

$$\lim_{r \to \infty} C(r) = C_b \tag{6}$$

then

$$C(\mathbf{b}, \mathbf{p}) = C_c + (C_B(t) - C_c)\left(1 - \frac{r_c}{d(\mathbf{b}, \mathbf{p})}\right) \tag{7}$$

where $d(\mathbf{b}, \mathbf{p})$ is the Euclidean distance between bacteria $\mathbf{b}$ and $\mathbf{p}$.

From equation 7, it is possible to find the radius for diffusion, $r_{dif}(t)$:

$$r_{dif}(t) = \frac{r_c - \frac{C_c}{C_B(t)}}{1 - \beta_C} \tag{8}$$

Since the model would be complicated by a non–constant radius, it is advantageous to use the following upper bound which is independent of C_B:

$$r_d = \frac{r_c}{1 - \beta_C} \tag{9}$$

This radius defines the spherical volume inside of which the model will consider the effect on antibiotic concentration of enzymatic degradation due to a producer cell at the center of the sphere. Beyond the border of the sphere, $C(\mathbf{b}, \mathbf{p}) < \beta_C C_B(t)$, and the effect of the enzyme producer is assumed to be negligible.

Due to the self–regulation of enzyme production, C_c will be constant even in situations with multiple producer bacteria within r_d of each other. In other words, when the spheres of influence of multiple producers overlap, each producer decreases its production of enzyme in such a way as to keep the antibiotic concentration at the cell wall at concentration C_c without wasting metabolic resources.

This implies that the effect of reduction in antibiotic concentration due to different producers is not cumulative. In this way, the net antibiotic concentration $C_{Net}(\mathbf{b})$ that would be experienced by a given bacterium $\mathbf{b}$ with multiple producer neighbors can be approximated as the concentration that would be experienced solely due to $\mathbf{p}_n$, the nearest producer bacterium:

$$C_{Net}(\mathbf{b}) = C(\mathbf{b}, \mathbf{n}_n) \tag{10}$$

Transcriptional regulation of the degradation enzyme's expression rate occurs over a timescale of minutes to hours [44], meaning that equilibrium levels of degradation are not reached immediately. The complete diffusion of antibiotic within the biofilm occurs within a similar time scale [45, 7]. The timestep chosen in this model is of similar magnitude. Because of this, the model assumes equilibrium levels of enzyme production and antibiotic diffusion are reached immediately.

2.3.3 Antibiotic Effect on Death

In spite of the fact that different classes of antibiotics differ in their mechanisms of action, it is widely reported that the effectiveness of an antibiotic decreases noticeably when cellular metabolism is slow, a feature at least partially responsible for the increased resistance of bacteria in biofilms to antibiotics when compared to their genetically identical, planktonic counterparts [9]. Furthermore, antibiotics, particularly β–lactams and other wall–targeting antibiotics, cause death only when the bacterium is undergoing growth, especially when it is attempting to undergo binary fission [5]. Because of this, antibiotic–induced death in this model is assumed to occur only upon attempting to undergo replication, as portrayed in Figure 1.

The probability of dying upon replication can be modeled using the Hill equation, originally developed as a model of enzyme–substrate interaction but frequently used within the domain of pharmacodynamics [46]. The probability of antibiotic–induced death at replication at a given antibiotic concentration of C would be given by:

$$P_{ad}(C) = \frac{1}{1 + \left(\frac{C_{1/2}}{C}\right)^h} \tag{11}$$

The discontinuity in equation 11 at $C = 0$ is removed by defining $P_{ad}(0) = 0$. In this equation, $C_{1/2}$ and h are parameters of the Hill equation, such that $P_{ad}(C_{1/2}) = 1/2$ and h describes the slope of the curve at $C = C_{1/2}$ [46]. In order to find values for $C_{1/2}$ and h, it is possible to use the experimentally determined values of C_M and C_I, more readily found in the literature for different

antibiotics. When $C = C_M$, there is no net growth. In the model described, at every replication attempt of a nonproducer bacteria, there are only two possible outcomes: antibiotic–induced death with probability P_{ab}, and successful replication with probability $1 - P_{ab}$. This means the expected value of population change $E[\Delta N]$ at every attempt at replication must be zero:

$$E[\Delta N] = -1 \cdot P_{ad}(C_M) + 1 \cdot (1 - P_{ad}(C_M)) = 0,$$
$$P_{ad}(C_M) = \frac{1}{2}.$$

Similarly, at $C = C_I$:

$$E[\Delta N] = -1 \cdot P_{ad}(C_I) + 1 \cdot (1 - P_{ad}(C_I)) = 1/2,$$
$$P_{ad}(C_M) = \frac{1}{4}.$$

Then solve for the value of h using $P_{ad}(C_I) = 1/4$:

$$C_{1/2} = C_M$$
$$h = \frac{\ln 3}{\ln\left(\frac{C_M}{C_I}\right)}$$

2.4 Population Density Effects

2.4.1 Density–Dependent Inhibition of Growth

It is well known that bacteria exhibit density–dependent population dynamics within biofilms [34, 14]. This phenomenon is well documented in biofilms, in which bacteria in deeper areas of the biofilm with less access to resources exhibit replication times many times slower than their surface–dwelling equivalents [14]. Given that resource limitation reduces metabolism, an assumption for this model is that density–dependent inhibition affects primarily probability of replication, rather than death. This assumption along with these density–dependent effects are accounted for in this model as a logistic term.

This logistic term is constructed from the maximum bacterial density in a given neighborhood sphere around a bacterium. Because nutrients and cellular waste products are also small molecules operating under similar diffusion kinetics as antibiotics, it is possible to assume the volume in which population density impacts a bacterium's growth is a sphere of radius r_d, as calculated above. For the same reason, the effect of new births and deaths within the sphere is assumed to be instantaneous

on the order of the time step chosen. The maximum density ρ_b can be calculated from the distance between bacteria in a tightly–packed biofilm using the sphere packing density relation:

$$\rho_b = \frac{\pi}{3\sqrt{2}} \cdot \frac{1}{\frac{4\pi}{3} {r_c}^3} = \frac{1}{4\sqrt{2} {r_c}^3}, \tag{12}$$

Then, the maximum number of bacteria in a given neighborhood sphere $N_{n,max}$ is given by:

$$N_{n,max} = \frac{4\pi}{3} {r_d}^3 \rho_b, \tag{13}$$

This value is then used to calculate the relative fitness of bacterium $\mathbf{b}$ due to population density in its neighborhood, $F_n(\mathbf{b})$, as a logistic term between 0 and 1. Here, relative fitness describes how likely it is for bacterium $\mathbf{b}$ to replicate when compared to a nonproducer bacterium in an antibiotic free environment with no resource limitation.

$$F_n(\mathbf{b}) = 1 - \frac{N_n(\mathbf{b})}{N_{n,max}}. \tag{14}$$

where $N_n(\mathbf{b})$ describes the number of neighbors of bacterium $\mathbf{b}$ within the neighborhood sphere of radius r_d.

2.4.2 Density–Dependent Enzyme Production

As has been mentioned before, bacteria that produce an antibiotic degradation enzyme invest metabolic resources that would otherwise be used in replication, resulting in reduced fitness when compared to nonproducer bacteria under equivalent conditions and absence of antibiotic [18]. Nevertheless, given that enzyme production is actively regulated and bacteria in a producer's neighborhood also benefit from its enzymatic degradation, enzyme production is decreased in communities with a large number of producers [7]. In this way, the fitness penalty associated with enzyme production is distributed among producer bacteria within a given neighborhood according to the distances between each producer. Thus, the relative fitness $F_e(\mathbf{b})$ of a producer bacterium $\mathbf{b}$ according to its own enzyme production and that of its $N_{pn}(\mathbf{b})$ producer neighbors, $prod(\mathbf{b})$, is given by:

$$F_e(\mathbf{b}) = 1 - \frac{1 - F_E}{N_{pn}(\mathbf{b}) + 1} \left(1 + \sum_{\mathbf{p} \in prod(\mathbf{b})} \frac{C(\mathbf{b}, \mathbf{p}) - C_c}{C_B(t) - C_c} \right) \tag{15}$$

Briefly, this expression divides the standard fitness penalty of producing enzyme $1 - F_E$ among the total number of producer bacteria in the neighborhood $N_{pn}(\mathbf{b}) + 1$, counting the producer $\mathbf{b}$. The

contribution of each neighboring producer is weighted according to the relative antibiotic concentration reduction of each case, where the relative contribution of bacteria **b** is equal to 1. Finally, the relative fitness is equal to the difference of 1 and the fitness penalty.

2.5 Probability of Replication and Death

The probabilities of replication and death both depend on the probability of attempting replication in a given time step t_s for bacterium **b**, $P_{ar}(\mathbf{b})$, which can be calculated based on all the above expressions:

$$P_{ar}(\mathbf{b}) = t_s \cdot \alpha_n \cdot F_n(\mathbf{b}) \cdot F_e(\mathbf{b}). \tag{16}$$

With this information, it is possible to calculate the probability of replication for bacterium **b** in time step t_s, $P_r(\mathbf{b})$ as the probability of attempting replication and not dying as a result of antibiotic exposure:

$$P_r(\mathbf{b}) = P_{ar}(\mathbf{b}) \cdot (1 - P_{ad}(\mathbf{b}))\,. \tag{17}$$

Nonproducer bacteria will generate nonproducer daughter cells upon successful replication. Producer bacteria will usually generate producer daughter cells, but they will occasionally generate nonproducer daughter cells upon replication with a probability of λ_L if all copies of the resistance plasmid remain inside one of the daughter cells due to random effects at replication [20].

On the other hand, the probability of death within a time step is given by the independent events of natural death and antibiotic–induced death at replication:

$$P_d(\mathbf{b}) = t_s\gamma_n + P_{ar}(\mathbf{b}) \cdot P_{ad}(\mathbf{b}) \tag{18}$$

If t_s is sufficiently small, it can be assumed that only one of the three possible events occurs every time step, and the event probabilities can be taken as independent.

2.6 Horizontal Gene Transfer

Horizontal gene transfer occurs through a variety of mechanisms, mainly uptake of free genetic material or transformation, viral transfection through bacteriophages, and conjugation [21]. This model accounts for all of these methods with the parameter λ_T. The probability of a nonproducer bacterium gaining producer status depends on the probability of uptake of the plasmid that encodes the gene for degradation enzyme. This probability of horizontal gene transfer is not considered in the case in which the bacterium is already a producer. However, a nonproducer bacterium has a probability

of acquiring resistance based on the population density of plasmid-bearing, producer bacteria in its neighborhood, as well as based on the rate of plasmid transfer. Thus, the probability $P_h(\mathbf{b})$ of a non-producer bacterium $\mathbf{b}$ switching phenotypes due to horizontal gene transfer during a given time step is:

$$P_h(\mathbf{b}) = \begin{cases} 0 & \mathbf{b} \in \text{Producer Bacteria} \\ t_s \lambda_T \cdot \frac{3N_{pn}(\mathbf{b})}{4\pi r_d^3} & \mathbf{b} \notin \text{Producer Bacteria} \end{cases} \tag{19}$$

2.7 Clustering Coefficients

Analysis was also done on the structure of the network to determine properties of the biofilm. The global clustering coefficient is defined as the number of closed connected triplets of nodes divided by the number of connected triplets, both opened and closed [47]. For a network with two classes of nodes (producer and nonproducer), this can be generalized to four coefficients which better capture the network topology, as shown in Figure 2. The Type I coefficient counts connected triplets of producer bacteria, while Type II captures the interaction of a nonproducer bacterium with surrounding resistant bacteria. Types III and IV are analogous but with the roles of producer and nonproducer bacteria switched. The included figures provide examples of the triplets that are counted. If the dashed line represents an edge, then the triplet is closed and will be included in the numerator of the corresponding coefficient.

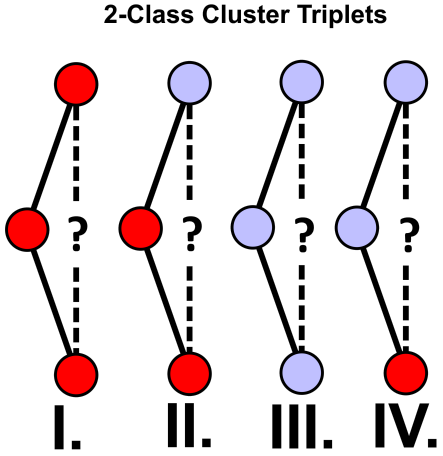

Figure 2: The four types of clustering coefficients. Type I is composed of all resistant bacteria and type III is composed of all susceptible bacteria. Dark red denotes producer bacteria, light blue denotes nonproducers.

2.8 Latin Hypercube Sampling

Latin Hypercube Sampling [48] was used to explore the parameter space of the model for three parameters of interest. Three parameters were chosen as descriptive of an antibiotic's mode of action: the minimum inhibitory concentration (C_M) for inhibiting visible bacterial growth, the 50% inhibitory concentration (C_I), and the relative fitness of a producer compared to a nonproducer (F_E). Biologically relevant ranges were selected for these parameters as obtained from the sources in 2, and Latin Hypercube Sampling was used to select various parameter values and combinations from within these ranges. Based on C_M antibiotic concentration values observed in literature, the range over which values were sampled for C_M was [1, 100]. Since the amount of antibiotic needed to inhibit 50% of bacterial growth should be less than the amount of antibiotic needed to inhibit 100% of bacterial growth, C_I should be a percentage of C_M. In order to calculate this C_I, random sampling was done over the interval [0.1, 0.9], and this value was multiplied by C_M for each Latin Hypercube Sampling trial. Finally, the value for bacterial fitness is between one and zero, and since enzyme production comes at a metabolic cost, the relative fitness of an enzyme–producing bacterium is less than one and greater than zero. Therefore, the range over parameter values for F_E were sampled was [0.1, 0.9]. Five random samples were generated from a uniform distribution over sections of each interval determined by Latin Hypercube Sampling using 5 divisions per parameter range. The parameter selections and combinations are given in Table 3.

Table 3: Latin Hypercube Samples

Sample	F_E	C_M	C_I
A	0.7321	17.8990	8.8390
B	0.5017	96.2564	75.9245
C	0.8692	59.5555	10.7284
D	0.4003	67.6231	44.2439
E	0.2271	35.0190	12.2136

2.9 Implementation and Simulation

The simulation was implemented in the C language (standard C99). Clustering analyses were carried out using Ruby and R scripts. Three-dimensional graphics were created using ParaView (https://www.paraview.org). The complete project source code is available on GitHub (https://github.com/bacteriaboyz/CheatingTheCheaters).

3 Results

Ten runs of the simulation under *P. aeruginosa*–piperacillin parameters were carried out, along with five random antibiotic sampling simulations. Visualization of the simulation exhibited clear clustering dynamics, with the bacteria forming into heterogeneous groups of producers and nonproducers once the antibiotic was applied, as seen in Figure 3. An animation of a given simulation of the *P. aeruginosa*–piperacillin system can be found at https://youtu.be/kJN0PWXCq1Y. Stable heterogeneous clusters occasionally spawned clusters of exclusively producers as the simulation progressed, leading to the growth of the population.

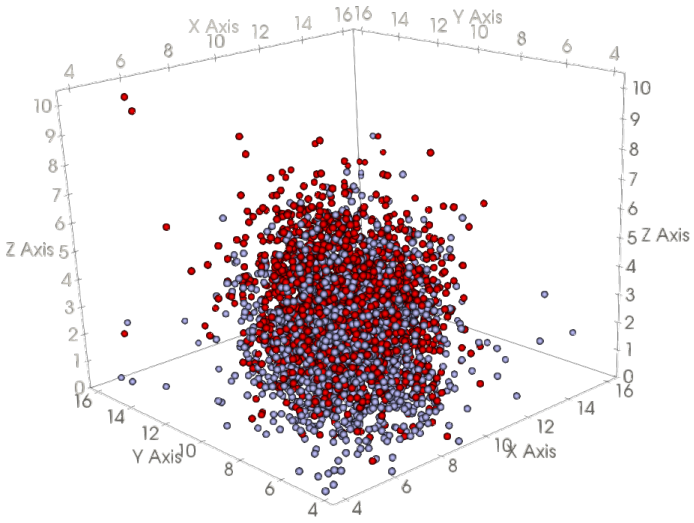

Figure 3: Simulation timeframe snapshot under the *P. aeruginosa*–piperacillin system (time 50 h). Dark red denotes producer bacteria, light blue denotes nonproducers.

3.1 *P. aeruginosa*–piperacillin system

The effects of the fitness cost for enzyme production are evident, as the bacterial population for producers remains much lower than that of logistically–growing nonproducers until the 12th hour, as can be seen in Figure 4. At this time, the first dose of antibiotic is introduced, and nonproducer bacteria start to die off. The restriction of growth could be seen in the simulation given that the concentration of the antibiotic confined the nonproducers within the vicinity of producers. Clusters of red and blue cells were heavily mixed, with the blue (nonproducers) located towards the interior of the producer cluster Figure 3. In terms of community structure, Figure 6 shows all clustering coefficients converged to the same value of $0.5 - 0.55$, indicating homogeneous community structure.

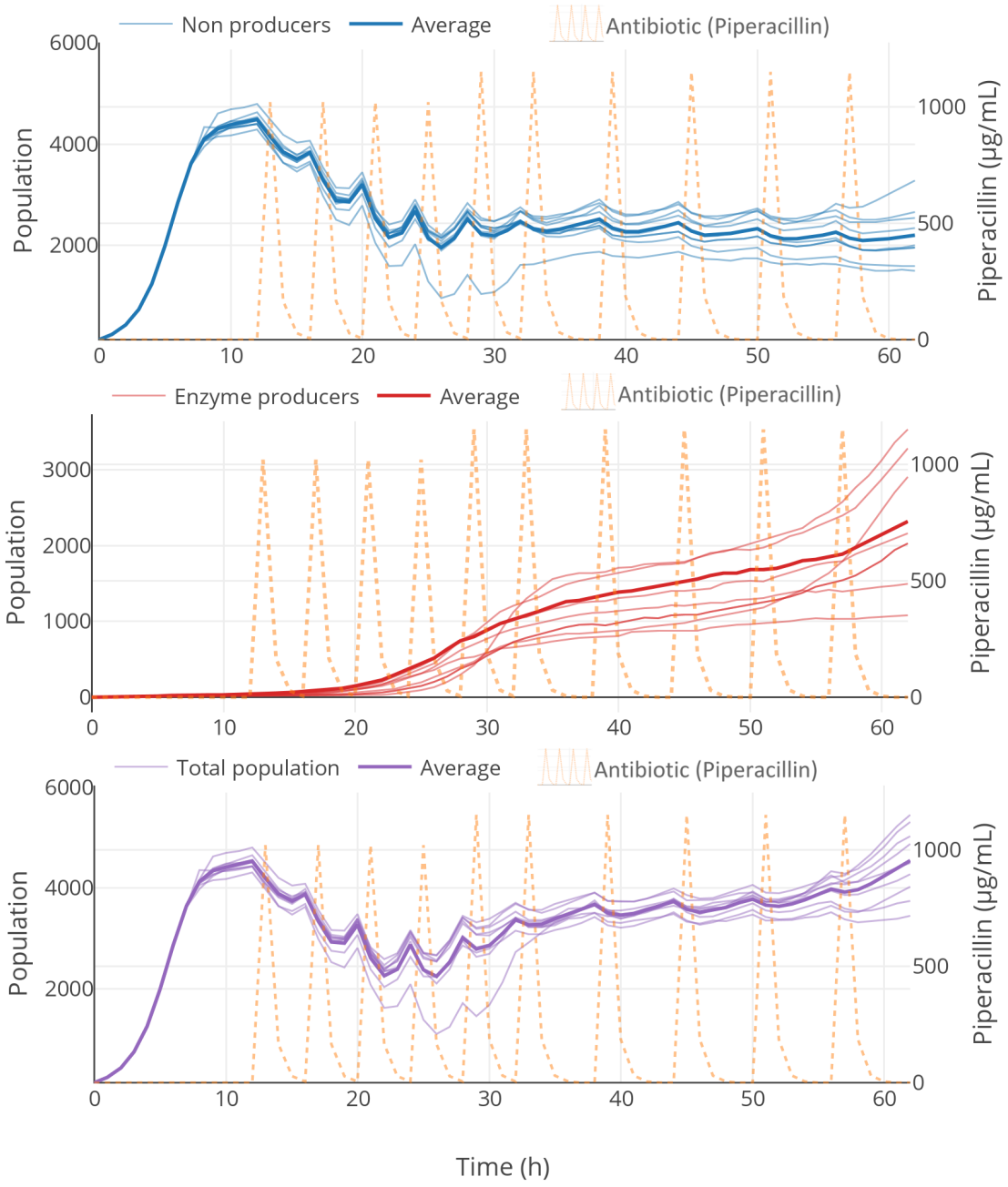

Figure 4: Population time series for the *P. aeruginosa*–piperacillin system.

3.2 Latin Hypercube Sampling

Variation of antibiotic variables yielded differing levels of producer final population, as seen in Figure 5. Particularly, parameter sets with low values of relative fitness for producers (high cost of producing degradation enzyme, $F_E < 0.6$) resulted in significantly lower producer populations. However, under

all conditions tested, the total community of the bacteria grew within the range of 3000 to 5000 bacteria by the end of the simulation. Even under conditions where the producer population was relatively low, the total bacteria population remained in this range. Unexpectedly, clustering coefficients exhibit convergence to roughly the same values as the previous case.

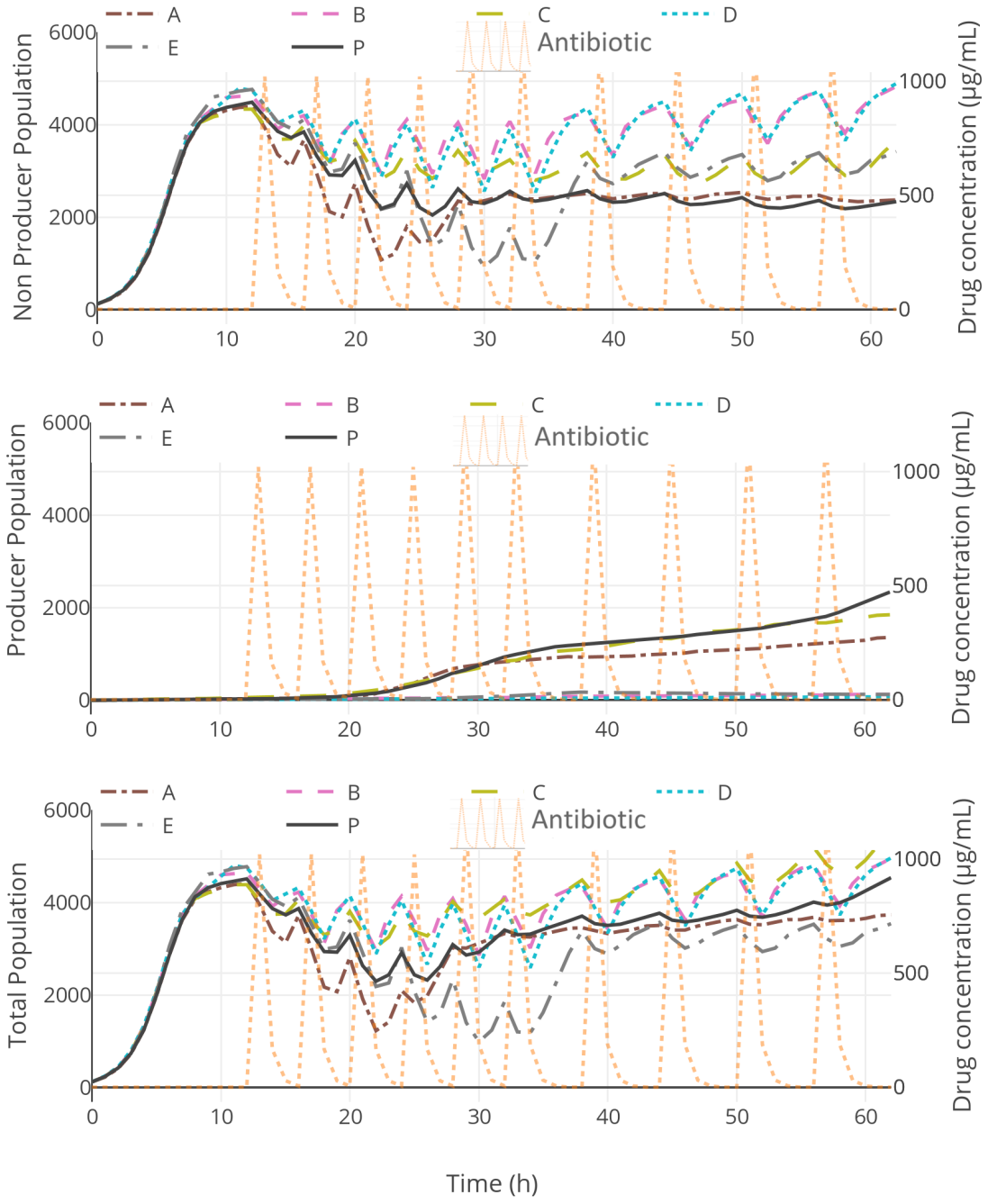

Figure 5: Population time series for the fictional antibiotics conceived through Latin Hypercube Sampling. The *P. aeruginosa*–piperacillin system average is shown in black for comparison.

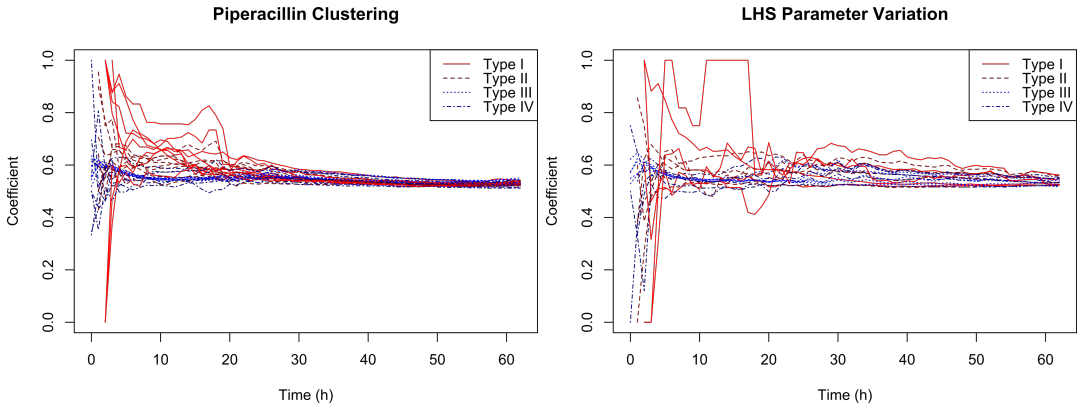

Figure 6: Clustering Coefficient Analysis

4 Discussion

While the simulation did not show the desired result of a total collapse of the bacterial community through competition, it did provide helpful insight into the relationship between producers and non-producers. This information can still be helpful in designing future treatment. The model reinforced the fact that antibiotic use can promote the growth of an antibiotic resistant population of bacteria [49]. This demonstrates that antibiotics, while necessary in confining bacterial spread, can significantly increase the lethality of bacterial disease, leading to the persistence of resistant cells. Such a scenario was shown in the simulation. While antibiotics helped in reducing resistant bacterial levels, it did not lead towards the collapse of the community and instead fostered the promotion of resistant cell. As a result, it can be induced that other key factors are affecting the longevity of the biofilm.

Additionally, the model exhibited another emergent behavior verified in experimental observations. For high population densities, bacteria show low probabilities of attempting reproduction and thus death rates due to the antibiotic are reduced. This explains why biofilms exhibit high levels of bacterial tolerance, even if the total population of producers is low. From the above, it can be concluded that if antibiotics are going to be implemented in an effort to cure resistant bacteria disease, the disease must be diagnosed early. At such an early phase, it is possible to considerably reduce the number of bacteria in the biofilm trough traditional antibiotic implementation, allowing the immune system to finish the bacteria off. Too late into the diagnosis and/or treatment schedule and the biofilm would have taken up a considerable amount. From then on it would prove expensive and dangerous to purse heavy antibiotic treatment without inducing a spike in resistant cell population. Moreover, the immune system would prove incapable of penetrated the protected barrier formed.

This density–dependence of antibiotic effectiveness also underscores the importance of a natural,

intrinsic bacterial death rate. Despite its low number, incorporating this rate allowed for the removal of bacteria from the biofilm. The open space provided nearby bacteria with an incentive to replicate. Doing so comes with the risk of antibiotic induced death, which makes population decrease possible. Interestingly, biofilms possess increased levels of autolysis through holin activation systems, as a mechanism of removing bacterial cells [25]. The process involves several bacterial cells releasing lysosomes that degrade several other bacteria inside the biofilm, and appears to be density–dependent as well, although it is still under experimental study. If true, this mechanism, once incorporated in the model, could increase the amount of antibiotic–induced death accounted for in simulations.

Out of the three parameters varied, the relative fitness of a producer bacterium was most critical to the survival of a resistant bacteria population. Drugs with $F_E < 0.6$ led to reduced levels of nonproducer bacteria. This is because the low fitness of a producer bacterium leads to lower replication rates compared to those of nonproducer cells. However, the producer cells were not driven to extinction by outcompetition from the nearby nonproducer cells. Instead, heterogeneous clumps were formed. In the presence of antibiotics, producer cells had a higher fitness than nonproducer cells, so they had higher replication rates. In addition, those very same neighboring resistance cells were able to share in the burden of enzyme production, increasing relative fitness. On the other hand, neighboring, nonproducer bacteria were sheltered from antibiotic concentration by being near their producer neighbors.

For these reasons, clustering was expected. The system exhibits high variation in the types of clustering that occur during the first hours of simulation, as shown in Figure 6. This is expected, given that small numbers of initial resistant bacteria account for large denominators and variation in clustering coefficients. Additionally, the absence of antibiotic implies that nonproducer bacteria can survive without producers in their neighborhood, allowing for greater variation in the clustering coefficients. After this initial period, they converge to a value, independently of the antibiotic parameters simulated. This can be explained in terms of stabilizing selection. There were two opposing selection pressures in this model. One selection pressure was resource limitation under population density, and the other selection pressure was antibiotic concentration. These two pressures were accounted for in $F_n(\mathbf{b})$ and $F_e(\mathbf{b})$, respectively. These terms affected probability of reproduction $P_{ar}(\mathbf{b})$, which in turn affected the probability of death, $P_d(\mathbf{b})$. The pressure of antibiotic concentration encouraged bacterial cells to clump near producers, and the selection pressure of population density encouraged bacteria not to clump too close together. These two selection pressures likely affected the clustering coefficient and the value at which it converged to. It remains to be seen why the convergence tends towards the given value specifically.

5 Conclusion

The model here proposed explores the spatial dynamics of resistance to antibiotics in heterogeneous populations of bacteria in a biofilm. The biofilm has proven resistant to treatment under various conditions. Mathematical and computational modeling prove that antibiotic treatment fosters resistance, as well as that high population density in biofilms results in lower metabolic rates and thus less susceptibility to antibiotics. These results highlight the importance of early treatment in bacterial disease, as well as the relevance of intrinsic death rates for the success of treatment. The clustering coefficient highlighted the relevance of selection pressures on biofilm formation, and its convergence under various parameter conditions highlighted the stability of the biofilm. the topology of the network played a key role in bacterial resistance. The clustering coefficient reflected how the network topology was a product of the selection pressures imposed on the bacteria population. Based on analysis of the model, treatment of a bacterial biofilm should involve using an antibiotic that leads to a high resistance cost for enzyme producing bacteria. Doing so would make their relative fitness, F_E, much lower compared to the fitness of nonresistant bacteria, which would lead to a lower total bacterial population in the patient. Of course, the fitness cost to the bacteria must also be compared with the cost to the patient in terms of side effects and potential lethality of the antibiotic treatment.

6 Future Work

Despite the information found through this study, much more research and query must be done to fully understand resistance in a biofilm. Previously, it was mentioned and explained why the clustering coefficients converged. However, it is not yet clear as to why it converges to 0.5-0.55 and not some other number above or below. Besides understanding why the clustering coefficients approach this value, it is important to ask if there is a way to change that value. Initial thoughts include using a graph theoretical/analytical approach to tackle both issues.

Along those same lines, the simulation shown resistant bacteria escape the main producer–nonproducer cluster and forming a small resistant cluster. The question becomes under what circumstances do resistant cells escape from the producer–nonproducer cluster and is there a way to prevent it. Understanding this problem can lead us into the overall goal of designing actual treatment schedules that lead to the collapse of the bacterial community without harming the patient.

Another avenue of research is studying further mechanisms of biofilm resistance. This paper highlighted biofilm resistance through the lens of stress response, assuming that antibiotics diffuse through

the film easily. However, that is not necessarily the case throughout the entire biofilm. Slow penetration is a biofilm property where the antibiotics outside the bacterial cells walls diffuses into the film at a slower rate due to the compactness of the cells near the outer. Some antibiotics may fail to penetrate due to the compactness of the surface cells. Other rates of resistance occur the deeper the antibiotics penetrates the biofilm. Beyond the region of stress response, the grouping of cells become more disperse. As the disparity/space increases the potency of antibiotics decrease. This region, often called an altered micro environment, continues to lower the concentration of antibiotics inside the biofilm. Finally, some biofilms possess an inner population of resistance cells used as a last line of defense for the preservation of the biofilm. This property has been termed as having an area of "persisters" [50]. Each one of these features has a profound effect on the concentration of antibiotic the biofilm comes into contact with, affecting bacterial fitness.

There are other treatments options that have yet to be implemented that made hold the key to solving the problem of bacterial resistance. They include applying a number of antibiotics concurrently on varying concentrations and dosages. Another method of treatments are using viruses called bacteriophages to disrupt the replication of bacterial cells. Finally, other strategies involves tackling the problem of anti–virulence instead of bacterial resistance.)

7 Supplementary Information

7.1 Simulation Pseudocode

Algorithm 1: Full Simulation

Data: Simulation parameters

Result: Spatial evolution of population size and composition over time

Setup (memory allocation, etc.);

Initialization (global variables);

for $t \leftarrow 0$ **to** t_{max} **do**

- UpdateAntibiotic(Simulation);
- **foreach** *b in bacteria* **do**
  - $random_1 \leftarrow Uniform(0, 1)$;
  - **if** $random_1 < P_r(b)$ **then**
    - Add b to replication stack;
  - **else if** $random_1 < P_r(b) + P_d(b)$ **then**
    - Add b to kill stack;
  - **else if** $random_1 < P_r(b) + P_d(b) + P_h(b)$ **then**
    - Add b to HGT stack;
- **foreach** *b in kill stack* **do**
  - KillBacterium(b);
- **foreach** *b in replication stack* **do**
  - ReplicateBacterium(b);
- **foreach** *b in HGT stack* **do**
  - HorizontalGeneTransfer(b);
- **foreach** *b in update stack* **do**
  - UpdateBacterium(b);
- Record simulation status;

Output results;

Algorithm 2: Initialize

Data: Simulation parameters

Result: Simulation environment under starting conditions

Initialize Biofilm with update set, replication, kill, and dead stacks ;

Add all bacteria to dead stack;

Initialize Simulation with Biofilm;

while *connected components > 1 and below iteration limit* **do**

  for $i \leftarrow 0$ **to** $\rho_b \cdot {X_{max}}^2 \cdot Z_{max} \cdot h_i$ **do**

    $isProducer \leftarrow 0$;

    if $Uniform(0,1) < t_s \phi_i, 0$ **then**

      $isProducer \leftarrow 1$

    $(x_r, y_r, z_r) \leftarrow (Uniform(0, X_{max}), Uniform(0, X_{max}), Uniform(0, Z_{max} \cdot h_i))$

    CreateBacterium$((x_r, y_r, z_r), isProducer, Simulation)$;

  Evaluate connectivity;

return Simulation

Algorithm 3: CreateBacterium

Data: Position, IsProducer, Simulation

Result: Bacterium added to Simulation at given position

Reinitialize unused Bacterium variable from dead stack;

Add new Bacterium into corresponding bucket;

$Potentialneighbors \leftarrow NearestNeighborStructure$;

foreach *pot in Potential neighbors* **do**

- $distance \leftarrow d(newbacterium, pot)$;
- **if** $distance < r_d$ **then**
  - Add pot and distance to new Bacterium from Nearest Neighbor Structure;
  - Add new Bacterium to neighbor's neighbor array;
  - Add distance from new Bacterium to neighbor's distance array;
  - Increase neighbor's number of neighbors by 1;
  - Add neighbor to update set if not there yet;

Add new Bacterium to update set;

return new Bacterium;

Algorithm 4: ReplicateBacterium

Data: Parent Bacterium, Simulation

Result: New Bacterium added to Simulation near parent

$isProducer \leftarrow parent.producer$;

if $Uniform(0, 1) < t_s \lambda_L$ **then**

- $isProducer \leftarrow$ **not** $isProducer$;

$(x_r, y_r, z_r) \leftarrow$ Random sphere sample around parent;

$daughter \leftarrow$ CreateBacterium$((x_r, y_r, z_r), isProducer, Simulation)$;

Algorithm 5: KillBacterium

Data: Bacterium,Simulation

Result: Bacterium set to unused in Simulation

Bacterium.used $\leftarrow 0$;

Check bucket index of Bacterium;

Remove Bacterium from bucket;

foreach *neighbor* $\in$ *Bacterium* **do**

    Remove Bacterium from neighbor's neighbor hash table;

    Reduce neighbor's number of neighbors by 1;

    Add neighbor to update set if not there yet;

Add Bacterium to dead stack;

Algorithm 6: HorizontalGeneTransfer

Data: Nonproducer Bacterium

Result: Bacterium producer status and HGT probability updated

Bacterium.producer $\leftarrow 1$;

foreach *n in neighbors* **do**

    Add neighbor to update set if not there yet;

Add Bacterium to update set if not there yet;

Algorithm 7: UpdateBacterium

Data: Bacterium

Result: Bacterium probabilities updated

-

Update $P_r(b)$;

Update $P_d(b)$;

Update $P_h(b)$;

Algorithm 8: UpdateAntibiotic

Data: Simulation,time

Result: Antibiotic concentration in total body water updated

$C_B \leftarrow C_B - \text{renalClearance}(C_B)$;

if $time \in T_d$ **then**

  $C_B \leftarrow C_B + D(time)$;

References

[1] Kaplan W and Lang R. Priority medicines for europe and the world. *World Health Organization: Department of Essential Drugs and Medicines Policy*, 2004.

[2] Philip S Brachman. Infectious diseases-past, present, and future, 2003.

[3] Viviane M Quirke. John Wiley and Sons, Ltd, 2001.

[4] Achievements in public health, 1900-1999: Control of infectious diseases.

[5] Webadmin. The antibiotic resistance crisis part 1: Causes and threats, Mar 2017.

[6] Julian Davies and Dorothy Davies. Origins and evolution of antibiotic resistance. *Microbiology and Molecular Biology Reviews*, 74(3):417–433, 2010.

[7] Marshall C Walters, Frank Roe, Amandine Bugnicourt, Michael J Franklin, and Philip S Stewart. Contributions of antibiotic penetration, oxygen limitation, and low metabolic activity to tolerance of pseudomonas aeruginosa biofilms to ciprofloxacin and tobramycin. *Antimicrobial agents and chemotherapy*, 47(1):317–323, 2003.

[8] Luanne Hall-Stoodley, J. William Costerton, and Paul Stoodley. Bacterial biofilms: from the natural environment to infectious diseases. *Nature Reviews Microbiology*, 2(2):95–108, 2004.

[9] Nicole M Vega and Jeff Gore. Collective antibiotic resistance: mechanisms and implications. *Current Opinion in Microbiology*, 21:28–34, 2014.

[10] Suriani Abdul Rani, Betsey Pitts, and Philip S Stewart. Rapid diffusion of fluorescent tracers into staphylococcus epidermidis biofilms visualized by time lapse microscopy. *Antimicrobial agents and chemotherapy*, 49(2):728–732, 2005.

[11] Philip S Stewart. Diffusion in biofilms. *Journal of bacteriology*, 185(5):1485–1491, 2003.

[12] Christopher Walsh et al. *Antibiotics: actions, origins, resistance.* American Society for Microbiology (ASM), 2003.

[13] KONG KOK-FAI, SCHNEPER LISA, and MATHEE KALAI. Beta-lactam antibiotics: from antibiosis to resistance and bacteriology. *APMIS*, 118(1):1 – 36, 2010.

[14] Lei Yang, Janus AJ Haagensen, Lars Jelsbak, Helle Krogh Johansen, Claus Sternberg, Niels Høiby, and Søren Molin. In situ growth rates and biofilm development of pseudomonas aeruginosa populations in chronic lung infections. *Journal of bacteriology*, 190(8):2767–2776, 2008.

[15] Niels Hoiby, Thomas Bjarnsholt, Michael Givskov, Soren Molin, and Oana Ciofu. Antibiotic resistance of bacterial biofilms. *International Journal of Antimicrobial Agents*, 35(4):322 – 332, 2010.

[16] Jed F. Fisher, Samy O. Meroueh, and Shahriar Mobashery. Bacterial resistance to beta-lactam antibiotics: Compelling opportunism, compelling opportunity. *Chemical Reviews*, 105(2):395–424, 2005. PMID: 15700950.

[17] Eugene A Yurtsev, Hui Xiao Chao, Manoshi S Datta, Tatiana Artemova, and Jeff Gore. Bacterial cheating drives the population dynamics of cooperative antibiotic resistance plasmids. *Molecular systems biology*, 9(1):683, 2013.

[18] Dan I Andersson and Bruce R Levin. The biological cost of antibiotic resistance. *Current Opinion in Microbiology*, 2(5):489 – 493, 1999.

[19] Howard Ochman. Lateral gene transfer and the history of bacterial genomes. 2006.

[20] Billy TC Lau, Per Malkus, and Johan Paulsson. New quantitative methods for measuring plasmid loss rates reveal unexpected stability. *Plasmid*, 70(3):353–361, 2013.

[21] John Davison. Genetic exchange between bacteria in the environment. *Plasmid*, 42(2):73 – 91, 1999.

[22] Kewal K. Jain. Future prospects of neuroprotective therapies. *The Handbook of Neuroprotection*, pages 529–531, 2011.

[23] Andras Szilagyi, Gergely Boza, and Istvan Scheuring. Analysis of stability to cheaters in models of antibiotic degrading microbial communities. *Journal of Theoretical Biology*, 423:53 – 62, 2017.

[24] R. F. Inglis, J. M. Biernaskie, A. Gardner, and R. Kümmerli. Presence of a loner strain maintains cooperation and diversity in well-mixed bacterial communities. *Proceedings of the Royal Society of London B: Biological Sciences*, 283(1822), 2016.

[25] Kenneth W Bayles. The biological role of death and lysis in biofilm development. *Nature reviews. Microbiology*, 5(9):721, 2007.

[26] Jing Luo, Jin-liang Kong, Bi-ying Dong, Hong Huang, Ke Wang, Li-hong Wu, Chang-chun Hou, Yue Liang, Bing Li, and Yi-qiang Chen. Baicalein attenuates the quorum sensing-controlled virulence factors of pseudomonas aeruginosa and relieves the inflammatory response in p. aeruginosa-infected macrophages by downregulating the mapk and nfκb signal-transduction pathways. *Drug design, development and therapy*, 10:183, 2016.

[27] Billy TC Lau, Per Malkus, and Johan Paulsson. New quantitative methods for measuring plasmid loss rates reveal unexpected stability. *Plasmid*, 70(3):353–361, 2013.

[28] Mikkel Klausen, Arne Heydorn, Paula Ragas, Lotte Lambertsen, Anders Aaes-Jorgensen, Soren Molin, and Tim Tolker-Nielsen. Biofilm formation by pseudomonas aeruginosa wild type, flagella and type iv pili mutants. *Molecular Microbiology*, 48(6):1511–1524, 2003.

[29] Eric P Widmaier, Hershel Raff, and Kevin T Strang. *Vander's human physiology*, volume 5. McGraw-Hill New York, NY, 2006.

[30] Xue Zhong, Jason Droesch, Randal Fox, Eva M Top, and Stephen M Krone. On the meaning and estimation of plasmid transfer rates for surface-associated and well-mixed bacterial populations. *Journal of theoretical biology*, 294:144–152, 2012.

[31] Rune Bakke, R Kommedal, and S Kalvenes. Quantification of biofilm accumulation by an optical approach. *Journal of Microbiological Methods*, 44(1):13–26, 2001.

[32] J Sjovall, D Westerlund, and G Alvan. Renal excretion of intravenously infused amoxycillin and ampicillin. *British journal of clinical pharmacology*, 19(2):191–201, 1985.

[33] U Frank, J Mutter, E Schmidt-Eisenlohr, and FD Daschner. Comparative in vitro activity of piperacillin, piperacillin–sulbactam and piperacillin–tazobactam against nosocomial pathogens isolated from intensive care patients. *Clinical microbiology and infection*, 9(11):1128–1132, 2003.

[34] David Lebeaux, Jean-Marc Ghigo, and Christophe Beloin. Biofilm-related infections: bridging the gap between clinical management and fundamental aspects of recalcitrance toward antibiotics. *Microbiology and Molecular Biology Reviews*, 78(3):510–543, 2014.

[35] Michael Cohen-Wolkowiez, Kevin M Watt, Chenguang Zhou, Barry T Bloom, Brenda Poindexter, Lisa Castro, Jamie Gao, Edmund V Capparelli, Daniel K Benjamin, and P Brian Smith. Developmental pharmacokinetics of piperacillin and tazobactam using plasma and dried blood spots from infants. *Antimicrobial agents and chemotherapy*, 58(5):2856–2865, 2014.

[36] Jason D Chambless, Stephen M Hunt, and Philip S Stewart. A three-dimensional computer model of four hypothetical mechanisms protecting biofilms from antimicrobials. *Applied and environmental microbiology*, 72(3):2005–2013, 2006.

[37] V Fanos and L Cataldi. Renal transport of antibiotics and nephrotoxicity: a review. *Journal of chemotherapy*, 13(5):461–472, 2001.

[38] F Sörgel and M Kinzig. The chemistry, pharmacokinetics and tissue distribution of piperacillin/tazobactam. *Journal of Antimicrobial Chemotherapy*, 31(suppl_A):39–60, 1993.

[39] Kimberly K Jefferson, Donald A Goldmann, and Gerald B Pier. Use of confocal microscopy to analyze the rate of vancomycin penetration through staphylococcus aureus biofilms. *Antimicrobial agents and chemotherapy*, 49(6):2467–2473, 2005.

[40] Cécile Morlot, André Zapun, Otto Dideberg, and Thierry Vernet. Growth and division of streptococcus pneumoniae: localization of the high molecular weight penicillin-binding proteins during the cell cycle. *Molecular microbiology*, 50(3):845–855, 2003.

[41] Hae-jin Woo, John Sanseverino, Chris D Cox, Kevin G Robinson, and Gary S Sayler. The measurement of toluene dioxygenase activity in biofilm culture of pseudomonas putida f1. *Journal of microbiological methods*, 40(2):181–191, 2000.

[42] Niels Bagge, Martin Schuster, Morten Hentzer, Oana Ciofu, Michael Givskov, Everett Peter Greenberg, and Niels Høiby. Pseudomonas aeruginosa biofilms exposed to imipenem exhibit changes in global gene expression and β-lactamase and alginate production. *Antimicrobial agents and chemotherapy*, 48(4):1175–1187, 2004.

[43] George H. Dibdin, Stephen J. Assinder, Wright W. Nichols, and Peter A. Lambert. Mathematical model of β-lactam penetration into a biofilm of pseudomonas aeruginosa while undergo-

ing simultaneous inactivation by released β-lactamases. *Journal of Antimicrobial Chemotherapy*, 38(5):757–769, 1996.

[44] Hakan Savli, Aynur Karadenizli, Fetiye Kolayli, Sibel Gundes, Ugur Ozbek, and Haluk Vahaboglu. Expression stability of six housekeeping genes: a proposal for resistance gene quantification studies of pseudomonas aeruginosa by real-time quantitative rt-pcr. *Journal of Medical Microbiology*, 52(5):403–408, 2003.

[45] Dirk de Beer, Paul Stoodley, Zbigniew Lewandowski, et al. Measurement of local diffusion coefficients in biofilms by microinjection and confocal microscopy. *Biotechnology and Bioengineering*, 53(2):151–158, 1997.

[46] Sylvain Goutelle, Michel Maurin, Florent Rougier, Xavier Barbaut, Laurent Bourguignon, Michel Ducher, and Pascal Maire. The hill equation: a review of its capabilities in pharmacological modelling. *Fundamental & clinical pharmacology*, 22(6):633–648, 2008.

[47] R Duncan Luce and Albert D Perry. A method of matrix analysis of group structure. *Psychometrika*, 14(2):95–116, 1949.

[48] Ronald L Iman. *Latin hypercube sampling*. Wiley Online Library, 2008.

[49] Philip S Stewart and J William Costerton. Antibiotic resistance of bacteria in biofilms. *The lancet*, 358(9276):135–138, 2001.

[50] Peter A Smith and Floyd E Romesberg. Combating bacteria and drug resistance by inhibiting mechanisms of persistence and adaptation. *Nature chemical biology*, 3(9):549–556, 2007.